

# Effect of Bismuth Additives on the Properties of Vanadium–Phosphorus Oxide Catalyst in the Partial Oxidation of *n*-Pentane

V. A. Zazhigalov

*Ukrainian–Polish Laboratory of Catalysis, Institute of Sorption and the Problems of Endoecology,  
National Academy of Sciences of Ukraine, Kiev, 03164 Ukraine*

Received November 23, 2000

**Abstract**—The selective oxidation of *n*-pentane on vanadium–phosphorus oxide (VPO) catalysts with bismuth additives ( $\text{Bi}/\text{V} = 0\text{--}0.30$ ) is studied. The catalysts are characterized by XRD, XPS, and specific surface area measurements using nitrogen adsorption. Their acidic properties are studied (using ammonia TPD and the 2-methyl-3-butyn-2-ol reaction). It was found that the introduction of bismuth insignificantly affects the specific surface area but increases the surface concentration of phosphorus and changes the acidic properties of the catalysts. The specific catalytic activity of samples in *n*-pentane oxidation correlates with the effective charge of surface oxygen ( $E_b$  of  $\text{O}1s$  electrons). The selectivity to citraconic anhydride increases with an increase in the general surface acidity. The selectivity to maleic anhydride increases with an increase in the Brønsted acidity of the surface. The selectivity to phthalic anhydride increases with an increase in the Lewis acidity. The pathways of product formation in the partial oxidation of *n*-pentane are proposed.

## INTRODUCTION

It is known that 50–60% of the cost of products obtained in the catalytic processes of hydrocarbon oxidation is determined by the cost of starting materials. Therefore, the oxidation of lower alkanes, which are cheap starting materials, attracts considerable attention from researchers. Progress achieved in *n*-butane oxidation to maleic anhydride, which substituted for benzene oxidation, motivated studies on the partial oxidation of *n*-pentane. Promising results were obtained in the first studies along these lines on vanadium–phosphorus oxide (VPO) catalysts [1–3] and demonstrated the possibility of obtaining a high yield of phthalic anhydride. More recent studies showed that the main product of *n*-pentane partial oxidation on VPO and other catalysts is maleic anhydride, whose amount in the products is higher than the amount of phthalic anhydride [4–10]. It has also been found that the ratio of these products depends on the state of the surface of a VPO catalyst [11, 12]. An attempt has been made to increase the efficiency of phthalic anhydride formation by adding iron and cobalt to these catalysts [13]. It has been shown that citraconic anhydride is formed along with other products of *n*-pentane oxidation on VPO catalysts [7, 8]. The formation of citraconic anhydride was confirmed in [9, 14]. The mechanism of *n*-pentane oxidation was debated in [2, 7, 9, 10, 14–18], but no agreement has been achieved on the pathways of product formation in the partial oxidation.

Note that, although the reaction of *n*-pentane oxidation is a promising alternative to *o*-xylene oxidation to phthalic anhydride, only one paper was devoted to the

effect of (Co and Fe) additives on the properties of a VPO system [13]. It is known that one of the most efficient promoters of VPO catalysts is bismuth, which enhances the selectivity to maleic anhydride in *n*-butane oxidation to maleic anhydride [19–21]. It has been shown that the addition of bismuth may play a positive role in *n*-pentane oxidation as well [7].

This study is devoted to the effect of bismuth concentration (at different  $\text{Bi}/\text{V}$  ratios) in a VPO catalyst on the selective oxidation of *n*-pentane.

## EXPERIMENTAL

Vanadium–phosphorus–bismuth oxide (VPBiO) samples were prepared in an organic solvent according to the procedure described earlier [22]. Bismuth was added together with  $\text{V}_2\text{O}_5$  in the form of  $\text{Bi}(\text{NO}_3)_3 \cdot 5\text{H}_2\text{O}$ . In the samples thus prepared, the P/V ratio was 1.15 and the  $\text{Bi}/\text{V}$  ratio ranged from 0 to 0.30. The active mass of the catalyst precursor was isolated by solvent evaporation and further drying at 250°C and a residual pressure of  $(2\text{--}4) \times 10^3$  Pa for 8 h. Then, the samples were pelleted and ground, and the 0.25–0.50 mm fraction was separated and used in catalytic tests.

Procedures for XRD and XPS characterization and data processing were described in [22].

The oxidation state of vanadium in the samples was determined by the method of double titration with  $\text{KMnO}_4$  using a procedure described in [23]. To determine the state of surface vanadium from XPS data, the values of binding energies of  $\text{V}2p_{3/2}$  electrons and an equation described in [24] were used.

The acidic properties of samples were determined using two methods: (1)  $\text{NH}_3$  adsorption from a flow of helium and its further TPD analysis by analogy with mass spectrometric analysis [25] and TPD curve decomposition on PC and (2) 2-methyl-3-butyn-2-ol (MBO) reaction at 180°C by analogy with [26]. It is known [26] that MBO transformation on acid sites occurs with the formation of 3-methyl-3-butene-1-yne (MBY) and 3-methyl-2-butene-1-al (MBA). Strong Lewis sites catalyze the formation of MBY, whereas Brønsted sites catalyze the formation of MBA [27]. Base sites are responsible for the formation of acetone and acetylene.

Before *n*-pentane oxidation experiments, all catalysts were activated in the process of *n*-butane oxidation (1.7 vol % in air) for 96 h at 440°C. The study of *n*-pentane (Fluka) oxidation was carried out using a setup at the Institute of Catalysis and Surface Chemistry, Polish Academy of Sciences (Cracow) in a steel reactor with an internal diameter of 6 mm. The reaction mixture contained 1.6 vol % of *n*-pentane in air. The flow rate was varied from 12 to 46  $\text{cm}^3/\text{min}$ . The catalyst loading was 0.5  $\text{cm}^3$ . The temperature was varied from 180 to 480°C. The initial mixture and reaction products were sampled using thermostatted (150–160°C) valves and analyzed by gas chromatography (a Chrom-5 chromatograph with PC recording). NaX zeolites were used for  $\text{O}_2$  and CO analysis with a 2-m column ( $T = 10\text{--}11^\circ\text{C}$ ) and a thermal conductivity detector (TCD); KSK-2.5 silica gel was used to analyze  $\text{CO}_2$  and hydrocarbons with a 3-m column ( $T = 50\text{--}150^\circ\text{C}$ , temperature-programmed mode) and TCD. Oxygenates were analyzed using two columns: Chromosorb (2.5-m column,  $T = 100\text{--}220^\circ\text{C}$ , temperature-programmed mode, TCD) for “mass-line” analyses of maleic and phthalic anhydrides and Porapak Q (3-m column,  $T = 100\text{--}220^\circ\text{C}$ , temperature-programmed mode, TCD) for the analyses of  $\text{C}_2\text{--C}_3$  acids and aldehydes.

The use of condensers after sampling valves made it possible to collect the reaction products and analyze them in solutions of acetone or acetonitrile. These analyses were carried out using a Varian 3400 chromatograph with a DB-1 capillary column coupled with an Incos-50 Finnigan mass spectrometer and used to determine possible intermediate products whose concentration can be lower than the GC sensitivity. Analyses were carried out periodically after accumulating the products for 4–5 h.

## RESULTS AND DISCUSSION

According to XRD data, all catalyst precursor samples contain the  $\text{VOHPO}_4 \cdot 0.5\text{H}_2\text{O}$  phase with intense reflections at  $d = 0.570$  (the maximal intensity), 0.451, 0.367, 0.329, 0.310, 0.294, 0.278, 0.265, and 0.185 nm. The bismuth-containing samples ( $\text{Bi}/\text{V} > 0.1$ ) had additional reflections at  $d = 0.442$ , 0.352, 0.303, 0.286, 0.245, and 0.216 nm corresponding to the  $\text{BiPO}_4$  phase. Their intensity increased with an increase in the amount of bismuth in the samples. After activation in the reaction of *n*-butane oxidation, the  $\text{VOHPO}_4 \cdot 0.5\text{H}_2\text{O}$  phase was replaced by the  $(\text{VO})_2\text{P}_2\text{O}_7$  phase in

**Table 1.** Specific surface area and acidic properties of VPBiO catalyst

Sample	Atomic Bi/V ratio	Specific surface area, $\text{m}^2/\text{g}$		Adsorption and $\text{NH}_3^*$ TPD		conversion, %	MBO reaction**	
		precursor	after catalysis	$A \times 10^6$ , $\text{mol}/\text{m}^2$	$C/A$		selectivity, mol %	MBY
VP-0	0	15.1	17.2	5.7	0.52	64	87	13
VP-5	0.050	12.2	14.3	6.4	0.50	80	88	12
VP-7.5	0.075	11.5	13.6	7.1	0.55	77	90	10
VP-10	0.100	12.5	14.1	8.4	0.57	79	90	10
VP-15	0.150	11.4	14.0	9.2	0.61	68	97	3
VP-17	0.170	11.0	13.0	9.3	0.61	72	96	4
VP-20	0.200	12.2	14.5	9.8	0.64	63	93	7
VP-25	0.250	11.6	14.7	9.7	0.65	61	89	11
VP-30	0.300	12.8	14.4	9.9	0.63	55	88	12
VP-35	0.350	11.5	14.0	6.3	0.52	49	82	18

\* Samples after catalysis;  $A$  is the general amount of desorbed ammonia, and  $C$  is the amount of ammonia desorbed at 250–500°C.

\*\* Samples after catalysis.

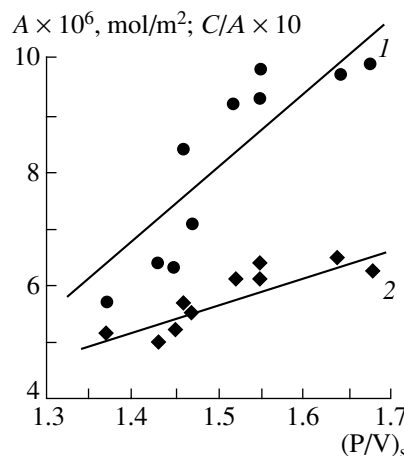


**Fig. 1.** Dependence of (1) amount of adsorbed ammonia ( $A$ ) and (2) the fraction of strongly adsorbed base ( $C/A$ ) on the atomic P/V ratio on the surface of VPBiO catalysts.

the XRD pattern. The latter was characterized by the reflections at  $d = 0.388$  (the maximal intensity), 0.313, 0.298, and 0.194 nm. The positions of  $\text{BiPO}_4$  reflections did not change upon activation.

As can be seen from data presented in Table 1, the introduction of bismuth into the VPO precursor results in a slight decrease of its specific surface area. The concentration of bismuth did not affect this characteristic. After activation and the catalytic reaction, an increase in the specific surface area was observed compared to the precursor. However, its value remains higher for the VPO than for VPBiO samples.

The results of chemical analyses of the samples (Table 2) show that the addition of bismuth to VPO catalysts did not change the oxidation state of vanadium, which is close to  $4+$ . The calculation of the oxidation state from XPS data according to the equation described in [24] overestimates this value in almost all cases. This can be due to the presence of excess oversstoichiometric phosphorus on the catalyst surface (Table 2). It is known that the binding energy of O1s electrons [28] in phosphorus pentoxide (533.8 eV) is much higher than in vanadium pentoxide. Correspondingly, the presence of excess phosphorus shifts the value of the binding energy of O1s electrons, and calculation based on the difference  $E_b$  (O1s – V2p) masks the true oxidation state of vanadium in the catalysts. We should also take into account a possible effect of OH groups and the donor–acceptor properties of the additive. The absolute values of binding energies of V2p electrons (Table 2) are constant and close to (517.3 eV). This value is characteristic of  $(\text{VO})_2\text{P}_2\text{O}_7$  [29] studied as a standard and containing  $\text{V}^{4+}$ .

As can be seen from Table 1, the addition of bismuth to the VPO catalyst results in an increase in the amount of adsorbed base (ammonia) pointing to an increase in the number of acid sites. A sample containing a substantial amount of Bi (VP-35, where 35 stands for the atomic Bi/V ratio) is an exception. In the thermal desorption of ammonia, no products of its oxidation were observed in agreement with earlier data for other VPO catalysts [30–32]. The partial oxidation of  $\text{NH}_3$  reported in [33] is associated with the presence of  $\text{V}^{5+}$  ions in substantial amounts, as mentioned by the authors of [33]. Ammonia oxidation on the vanadium

**Table 2.** Results of analyses of VPBiO catalysts by XPS

Sample	Binding energy, eV			$(\text{P/V})^*$	Vanadium oxidation state	
	V2p	P2p	O1s		calculation by equation from [24]	chemical analysis
VP-0	517.2	133.8	531.5	1.37	4.10	3.98
VP-5	517.1	133.7	531.5	1.43	4.03	3.97
VP-7.5	517.3	133.8	531.4	1.47	4.23	4.02
VP-10	517.2	133.8	531.4	1.46	4.16	3.96
VP-15	517.1	133.9	531.3	1.52	4.16	3.89
VP-17	517.2	133.7	531.2	1.55	4.30	3.96
VP-20	517.4	133.9	531.3	1.55	4.37	4.04
VP-25	517.1	133.6	531.4	1.64	4.10	4.02
VP-30	517.3	133.7	531.5	1.68	4.16	3.96
VP-35	517.1	133.8	531.6	1.45	3.96	4.05

\* Surface atomic P/V ratio.

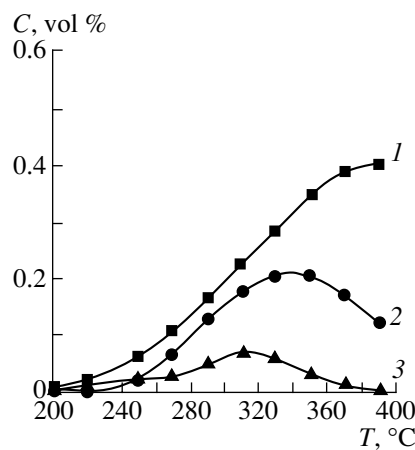


**Fig. 2.** Dependence of the concentration of (1) maleic, (2) phthalic, and (3) citraconic anhydrides on the temperature of *n*-pentane oxidation on the VPBiO (VP-20) catalyst ( $\tau_c = 1.4$  s).

phosphate phase containing  $V^{5+}$  was also demonstrated in [34]. Note that, with the exception of the VP-35 sample, an increase in the concentration of bismuth in the catalyst leads to an increase in the relative fraction of sites for strong base adsorption (strong acid sites). Figure 1 shows a good correlation of the amount of adsorbed ammonia, its strongly bound state, and the atomic P/V ratio on the catalyst surface. One might conjecture that a change in the acidity with the addition of bismuth is associated with an increase in the number of POH groups. However, results obtained in the study of the MBO reaction (Table 1) show that the dependence of the number of Brønsted sites (the selectivity to

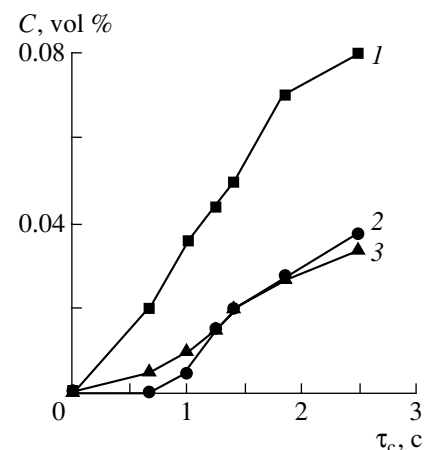


**Fig. 3.** Dependence of the concentration of (1) maleic, (2) phthalic, and (3) citraconic anhydrides on the contact time in *n*-pentane oxidation on the VPBiO (VP-20) catalyst ( $T = 250$  °C).

MBA) on the amount of bismuth in the catalyst has an extremum.

The products of partial oxidation of *n*-pentane contained maleic, phthalic, and citraconic anhydrides (the main products), acetic and acrylic acids,  $C_4$  olefins, and butadiene. Mass spectrometric analysis also showed the presence of pentanol(s), benzoic acid, and tetrahydrophthalic anhydride in trace amounts. Figure 2 shows changes in the concentrations of the main products of partial oxidation of *n*-pentane on temperature for the VP-20 catalyst (analogous dependences were observed on other samples as well). As can be seen from these data, maleic and citraconic anhydrides are mainly

**Table 3.** Properties of the VPBiO catalyst in *n*-pentane oxidation (300°C,  $\tau_c = 1.4$  s)

Sample	Conversion, %	Oxidation rate, $w \times 10^4$ , mol $h^{-1} m^{-2}$	Selectivity*, mol %		
			MA	PA	CA
VP-0	21.2	0.34	42.4	18.7	0
VP-5	22.9	0.42	40.5	20.4	1.8
VP-7.5	25.3	0.47	37.1	24.9	4.7
VP-10	27.6	0.52	36.6	26.1	6.8
VP-15	30.2	0.62	32.4	36.8	10.4
VP-17	34.8	0.71	31.9	35.5	10.1
VP-20	37.5	0.68	35.7	29.8	11.2
VP-25	36.4	0.61	40.1	25.3	11.7
VP-30	35.9	0.63	41.4	22.5	10.9
VP-35	24.7	0.44	44.7	15.4	2.7

\* MA is maleic anhydride, PA is phthalic anhydride, and CA is citraconic anhydride.

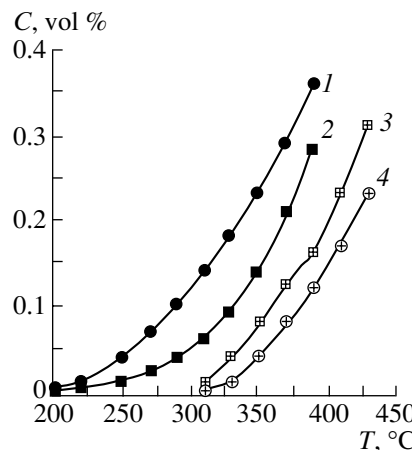


**Fig. 4.** Dependence of the concentration of deep oxidation products on the temperature in the reaction with the participation of *n*-pentane (1)  $\text{CO}_2$ , (2)  $\text{CO}$  and *n*-butane (3)  $\text{CO}_2$ , (4)  $\text{CO}$  on the VPBiO (VP-20) catalyst ( $\tau_c = 1.4$  s).

formed at low temperatures. With an increase in temperature ( $\Delta T = 20\text{--}30^\circ\text{C}$ ), phthalic anhydride appears in the reaction products. An analogous phenomenon was noted for the dependence of the concentrations of anhydrides on the contact time at a constant reaction temperature (Fig. 3). As can be seen, maleic and citraconic anhydrides are formed at short contact times ( $\tau_c$ ) and phthalic anhydride is formed at longer contact times.

Note that, over the whole studied range of temperatures, the concentration of maleic anhydride in the reaction products is higher than the concentration of phthalic anhydride. The dependence of the citraconic and phthalic anhydride concentrations on temperature has extrema. For the first of these dependences, the maximum is observed at a lower temperature. The presence of a maximum for the concentration of the citraconic anhydride ( $310\text{--}320^\circ\text{C}$ ) can be explained by its oxidation to maleic anhydride. In the case of phthalic anhydride, the presence of a maximum at  $350\text{--}360^\circ\text{C}$  can hardly be explained by its further oxidation, because it is known to form with a maximal selectivity at much higher temperatures in *o*-xylene oxidation [35]. Our studies on the oxidation of phthalic anhydride (0.6–0.7 vol %) by air on the VP-10 catalyst showed that the reaction starts at a noticeable rate at  $380\text{--}390^\circ\text{C}$ .

In the products of deep oxidation of *n*-pentane, the amount of  $\text{CO}_2$  was higher than the amount of  $\text{CO}$  at all temperatures studied. This means that this reaction differs from *n*-butane oxidation, where excess  $\text{CO}$  is observed (Fig. 4).

Table 3 shows that the addition of bismuth to the VPO catalyst leads to an increase in the conversion of *n*-pentane and its specific rate of oxidation. The maximal conversion of the alkane is achieved for the samples with an atomic  $\text{Bi}/\text{V}$  ratio of 0.20–0.25, and the maximal specific rate is achieved for the samples with a  $\text{Bi}/\text{V}$  ratio of 0.17–0.20. On the other hand, Fig. 5 shows that the specific rate of oxidation correlates with

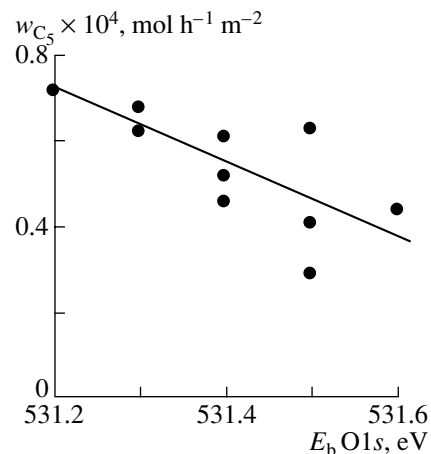


**Fig. 5.** Dependence of the specific rate of *n*-pentane oxidation on the VPBiO catalysts on the binding energy of O1s electrons of sample surfaces.

the binding energy of O1s electrons on the catalyst surface. The rate of *n*-pentane oxidation increases with a decrease in  $E_b$  for O1s, that is, with an increase in the effective negative charge on the surface oxygen atoms. Similar correlations were observed earlier for the oxidation of propane [36] and *n*-butane [37].

As Table 3 shows, the addition of bismuth to the VPO catalyst changes the selectivity to *n*-pentane oxygenates. Due to the addition of bismuth, a sample that was inactive toward the formation of citraconic anhydride starts to show activity. The dependence of the selectivity to the anhydride on the concentration of bismuth in the sample has an extremum (a maximum at  $\text{Bi}/\text{V} = 0.20\text{--}0.25$ ). Figure 6 illustrates an increase in the selectivity to citraconic anhydride with an increase in the fraction of acid sites ( $C/A$ ) on the catalyst surfaces. An analogous relationship was observed for the selectivity and the number of strong acid sites ( $C$ ).

The selectivity to maleic anhydride decreases when bismuth is added and decreases with an increase in the additive concentration to  $\text{Bi}/\text{V} = 0.17$ . With a further increase in the concentration of bismuth in the sample, an increase in the selectivity to maleic anhydride is observed. The dependence of the selectivity to phthalic anhydride on the concentration of bismuth in the catalyst has an “inversion nature”: initially, it increases and then starts to decrease at  $\text{Bi}/\text{V} > 0.17$ . Data summarized in Tables 1 and 3 show the absence of correlation between the selectivities to maleic and phthalic anhydrides and the parameters of surface acidity determined by adsorption and ammonia TPD tests. However, comparison of data on the selectivity with the results obtained in the MBO reaction demonstrates that there is good correlation between these parameters (Fig. 7). It follows from this figure that the selectivity to maleic anhydride decreases with an increase in the selectivity to MBY that characterizes the presence of strong Lewis

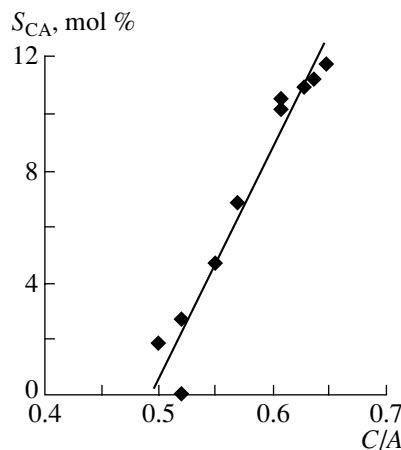
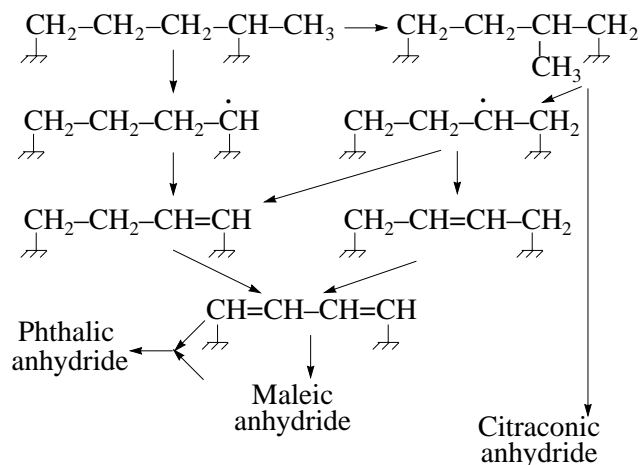


Fig. 6. Dependence of the selectivity to citraconic anhydride in the oxidation of *n*-pentane on the VPBiO catalysts on the fraction of strong acid sites of the surface ( $C/A$ ).

sites. The selectivity to phthalic anhydride increases with an increase in the number of sites of this type.

The results obtained allow us to propose the general scheme of *n*-pentane transformation to oxygenates on VPBiO catalysts:



Proceeding from this scheme and using an analogy with the mechanism of *n*-butane conversion on  $(\text{VO})_2\text{P}_2\text{O}_7$  considered earlier [38–42], the activation of a pentane molecule occurs with proton abstraction from the first and fourth carbon atoms ( $\text{C}_1$  and  $\text{C}_4$ ) and their fixation at oxygen on the catalyst surface (vanadyl oxygen). The dependence of the specific rate of oxidation on the effective negative charge at the oxygen atom (Fig. 5) provides evidence for this. The presence of strong acid sites on the surface favors the isomerization of a hydrocarbon fragment and its oxidation to citraconic anhydride. The dependence of the selectivity to this product on the fraction of strong acid sites is shown in Fig. 6. The abstraction of the methyl group leads to the formation of an unstable  $\text{C}_4$  radical. It is known that such radicals readily transform into  $\text{C}_4$  olefins or are oxidized to  $\text{CO}_x$  (mostly  $\text{CO}_2$ ) [43]. Olefin structures

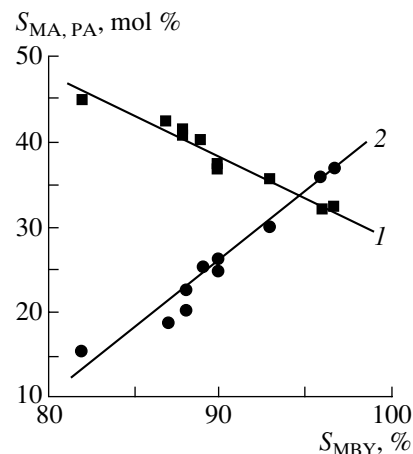


Fig. 7. Dependence of the selectivity to (1) maleic and (2) phthalic anhydrides in the oxidation of *n*-pentane on the VPBiO catalysts on the selectivity to MBY in the reaction of MBO on these samples.

formed in the reaction are further oxidized to maleic anhydride via the known mechanism [39, 40, 44, 45]. An increase in the Brønsted acidity of the surface favors the desorption of this product and increase the selectivity to it (Tables 1 and 3; Fig. 7). On the other hand, in the oxidation of olefins  $\text{C}_4$ , the amount of  $\text{CO}_2$  in the reaction products is higher than the amount of  $\text{CO}$ . This can explain the regularities of formation of the deep oxidation products and their difference from the process of *n*-butane oxidation (Fig. 4). The formation of phthalic anhydride occurs via the Diels–Alder reaction between the maleic anhydride and diolefin (olefin) structures  $\text{C}_4$ . It is known that the Diels–Alder reaction with the participation of butadiene occurs in the forward direction at 250–330°C [46], unlike the process with the participation of olefins  $\text{C}_5$ , which only occurs at low temperatures. This mechanism of phthalic anhydride formation is also supported by the dependences of product formation (Figs. 2 and 3) from which we see that phthalic anhydride appears in the products at higher temperatures and contact times than maleic anhydride. That is, the formation of phthalic anhydride occurs when the reactants contain necessary amounts of maleic anhydride and olefin  $\text{C}_4$  structures. It is noteworthy that temporal analysis of products also showed that phthalic anhydride is formed after maleic anhydride in *n*-pentane oxidation, although they are formed simultaneously in the oxidation of olefin  $\text{C}_5$  [17]. The presence of tetrahydrophthalic anhydride, which is oxidized to phthalic anhydride with a high selectivity [47], in the products of *n*-pentane oxidation determined in this work by mass spectroscopic analysis also provides evidence for the Diels–Alder reaction. The presence of a maximum for the concentrations of phthalic anhydride at these low temperatures can be explained by the process limited by a low stationary concentration of olefins  $\text{C}_4$ , which are oxidized to maleic anhydride in parallel, or by the reversibility of the Diels–Alder reac-

tion at high temperatures. The presence of the relation between the selectivity to phthalic anhydride and Lewis acidity (Fig. 7) can be associated with the stabilization of adsorbed olefin structures on the sites of this sort. According to the data obtained in this work, the selectivity to phthalic anhydride is determined by different sites of the VPO catalyst surface, and this agrees with conclusions drawn in [10].

Thus, our studies of the effect of bismuth additives on the properties of the VPO catalyst in the reaction of *n*-pentane oxidation showed the possibility of increasing the selectivity to the partial oxidation products and promising methods of selectivity control. Enhancing the general acidity and the strength of acid sites of the catalyst can lead to an increase in the selectivity to citraconic anhydride. The selectivity to maleic anhydride increases with an increase in the Brønsted acidity, and the selectivity to phthalic anhydride increases with an increase in the Lewis acidity of the catalyst surface.

#### ACKNOWLEDGMENTS

I thank Dr. M. Genser (Institute of Catalysis and Surface Chemistry, Polish Academy of Sciences, Cracow) for mass spectrometric analysis, Dr. I.V. Bacherikova for XPS studies of the catalyst samples, and Dr. S.B. Grinenko for the thermal desorption mass spectrometric studies of NH<sub>3</sub>. Financial support from ISEP (grant no. QSU083065) is acknowledged.

#### REFERENCES

1. Centi, G., Burattini, M., and Trifiro, F., *Appl. Catal.*, 1987, vol. 32, no. 2, p. 353.
2. Centi, G. and Trifiro, F., *Chem. Eng. Sci.*, 1990, vol. 45, no. 8, p. 2589.
3. Centi, G., Lopez Nieto, J., Pinelli, D., Trifiro, F., and Ungarelli, F., *Stud. Surf. Sci. Catal.*, 1990, vol. 55, p. 635.
4. Sobalik, Z., Gonzalez, S., and Ruiz, P., *Stud. Surf. Sci. Catal.*, 1995, vol. 91, p. 727.
5. Michalakos, P.M., Birkeland, K., and Kung, H.H., *J. Catal.*, 1996, vol. 158, no. 2, p. 349.
6. Ozkan, U.S., Gooding, R.E., and Schilf, B.T., *Heterogeneous Hydrocarbon Oxidation* (211th ACS National Meeting), New Orleans, 1996, vol. 41, no. 1, p. 176.
7. Zazhigalov, V.A., Haber, J., Stoch, J., Mikhajluk, B.D., Pyatnitskaya, A.I., Komashko, G.A., and Bacherikova, I.V., *Catal. Lett.*, 1996, vol. 37, no. 1, p. 95.
8. Zazhigalov, V.A., Mikhailyuk, B.D., Stokh, E., Bacherikova, I.V., Golovaty, V.G., and Shabel'nikov, V.P., *Teor. Eksp. Khim.*, 1996, vol. 32, no. 3, p. 186.
9. Ozkan, U.S., Harris, T.A., and Schilf, B.T., *Catal. Today*, 1997, vol. 33, no. 1, p. 57.
10. Sobalik, Z., Gonzalez Carrazan, S., Ruiz, P., and Delmon, B., *J. Catal.*, 1999, vol. 185, no. 2, p. 272.
11. Calestani, G., Cavani, F., Duran, A., Mazzoni, G., Stefanini, G., Trifiro, F., and Venturoli, P., *Stud. Surf. Sci. Catal.*, 1995, vol. 92, p. 179.
12. Albonetti, S., Cavani, F., Trifiro, F., Venturoli, P., Calestani, G., Lopez Granados, M., and Fierro, J.L.G., *J. Catal.*, 1966, vol. 160, no. 1, p. 52.
13. Cavani, F., Colombo, A., Trifiro, F., Sananes Schulz, M.T., Volta, J.C., and Hutchings, G.J., *Catal. Lett.*, 1997, vol. 43, no. 3, p. 241.
14. Cavani, F., Colombo, A., Giuntoli, F., Gobbi, E., Trifiro, F., and Vazquez, P., *Catal. Today*, 1996, vol. 32, no. 1, p. 125.
15. Busca, G. and Centi, G., *J. Am. Chem. Soc.*, 1989, vol. 111, no. 1, p. 46.
16. Centi, G., Golinelli, G., and Busca, G., *J. Phys. Chem.*, 1990, vol. 94, no. 17, p. 6813.
17. Golinelli, G. and Gleaves, J.T., *J. Mol. Catal.*, 1992, vol. 73, no. 3, p. 353.
18. Cavani, F. and Trifiro, F., *Appl. Catal.*, 1997, vol. 157, nos. 1–2, p. 195.
19. Hutchings, G., *Appl. Catal.*, 1991, vol. 72, no. 1, p. 1.
20. Yamazoe, N., Morishige, H., Tamaki, J., and Miura, N., *Stud. Surf. Sci. Catal.*, 1993, vol. 75, p. 1989.
21. Ruiz, P., Bastians, Ph., Caussin, L., Reuse, R., Dasa, L., Acosta, D., and Delmon, B., *Catal. Today*, 1993, vol. 16, no. 1, p. 99.
22. Zazhigalov, V.A., Haber, J., Stoch, J., Pyatnitskaya, A.I., Komashko, G.A., and Belousov, V.M., *Appl. Catal.*, 1993, vol. 96, no. 1, p. 135.
23. Hodnett, B.K., Permanne, Ph., and Delmon, B., *Appl. Catal.*, 1983, vol. 6, no. 2, p. 231.
24. Coulston, G.W., Thompson, E.A., and Herron, N., *J. Catal.*, 1996, vol. 163, no. 1, p. 122.
25. Stoch, J., Podobinski, J., and Zazhigalov, V.A., Abstracts of Papers, *EUROPACAT-IV*, Rimini, 1999, p. 671.
26. Lauron-Pernot, H., Luck, F., and Popa, J.M., *Appl. Catal.*, 1991, vol. 78, no. 2, p. 213.
27. Audry, F., Hoggan, P.E., Saussey, J., Lavalley, J.C., Lauron-Pernot, H., and Le Govic, A.M., *J. Catal.*, 1997, vol. 168, no. 2, p. 471.
28. Nefedov, V.I. *Rentgenoelektronnaya spektroskopiya khimicheskikh soedinenii* (X-ray Electron Spectroscopy of Chemical Compounds), Moscow: Khimiya, 1984.
29. Zazhigalov, V.A., Konovalova, N.D., and Stokh, E., *Kinet. Katal.*, 1988, vol. 29, no. 2, p. 419.
30. Busca, G., Centi, G., Trifiro, F., and Lorenzelli, V., *J. Phys. Chem.*, 1986, vol. 90, no. 7, p. 1337.
31. Satsuma, A., Hattori, A., Furuta, A., Miyamoto, A., Hattori, T., and Murakami, Y., *J. Phys. Chem.*, 1988, vol. 92, no. 12, p. 2275.
32. Ruiz, P., Bastians, Ph., Caussin, L., Reuse, R., Dasa, L., Acosta, D., and Delmon, B., *Catal. Today*, 1993, vol. 16, no. 1, p. 99.
33. Berndt, H., Bunker, K., Martin, A., Bruckner, A., and Lucke, B., *J. Chem. Soc., Faraday Trans.*, 1995, vol. 91, no. 5, p. 725.
34. Centi, G. and Perathoner, S., *J. Catal.*, 1993, vol. 142, no. 1, p. 84.
35. Nikolov, V., Klissurski, D., and Anastasov, A., *Catal. Rev.-Sci. Eng.*, 1991, vol. 33, no. 3, p. 319.
36. Sokolovskii, V.D., *Catal. Rev.-Sci. Eng.*, 1990, vol. 32, no. 1, p. 1.

37. Zazhigalov, V.A., Haber, J., Stoch, J., Bacherikova, I.V., Komashko, G.A., and Pyatnitskaya, A.I., *Appl. Catal., A*, 1996, vol. 134, no. 2, p. 225.
38. Novak, Ya. and Gerei, Sh., *Geterogennyi kataliz* (Heterogeneous Catalysis), Sofia: Bulgar. Akad. Nauk, 1983, vol. 1, p. 171.
39. Ziolkowski, J., Bordes, E., and Courtine, P., *J. Catal.*, 1990, vol. 122, no. 1, p. 126.
40. Ziolkowski, J., Bordes, E., and Courtine, P., *J. Mol. Catal.*, 1993, vol. 84, no. 2, p. 307.
41. Zazhigalov, V.A., *Heterogeneous Hydrocarbon Oxidation* (211th ACS National Meeting), New Orleans, 1996, vol. 41, no. 1, p. 207.
42. Zazhigalov, V.A., *Teor. Eksp. Khim.*, 1999, vol. 35, no. 5, p. 265.
43. Chakir, A., Cathonnet, M., Boettner, J.C., and Gaillard, F., *Combust. Sci. Tech.*, 1989, vol. 65, no. 2, p. 207.
44. Centi, G., Trifiro, F., Ebner, J.R., and Franchetti, V.M., *Chem. Rev.*, 1988, vol. 88, no. 1, p. 55.
45. Seeboth, H., Kubias, B., Wolf, H., and Lucke, B., *Chem. Tech.*, 1978, vol. 28, no. 7, p. 730.
46. Ingold, C.K., *Structure and Mechanism in Organic Chemistry*, Ithaca: Cornell Univ., 1969.
47. Centi, G., Lopez Nieto, J., Ungarelli, F., and Trifiro, F., *Catal. Lett.*, 1990, vol. 4, no. 3, p. 309.